

EFFECTS OF WALL ROUGHNESS ON PRESSURE  
LOSS AND VELOCITY DISTRIBUTION FOR AIR  
IN FIXED AND MOVING GRANULAR LAYERS

V. K. Durnov and V. N. Timofeev\*

UDC 532.546

Increase in friction between the material and the wall under counterflow conditions is accompanied by a reduction in the pressure loss and an increase in the nonuniformity of the gas flow in a horizontal cross section of the bed.

The proportion of a granular material in effective contact with the wall is usually expressed via the geometrical ratio  $d/D$  and is governed by a number of factors [1-4].

The effects of the geometrical simplex on the pressure loss have been examined [5-7], but these studies were for a stationary layer; if one has a moving close-packed gravitational layer, one gets a layer near the wall with distorted open structure whose thickness is largely dependent on the friction between the material and the wall [8-13]. It is also clear that the porosity of the layer as a whole will also be dependent on the wall roughness. Both of these factors should be reflected in the total pressure loss and in the distribution of the gas flow in a horizontal cross section of a bed if one varies the coefficient of friction.

Consider a layer consisting of two parts: one near the wall and a central one, which differ in packing density. We assume that the pressure distribution is the same throughout the cross section, and then

$$\Delta P_w = \Delta P_c = \Delta P. \quad (1)$$

We give as follows the pressure loss over the various parts:

$$\Delta P_w = \lambda \frac{h}{D} \cdot \frac{\gamma V_w^2}{2g}, \quad (2)$$

$$\Delta P_c = \zeta \frac{h}{d} \cdot \frac{\gamma V_c^2}{2g}. \quad (3)$$

Also, general considerations give that

$$F = F_w + F_c; \quad W = W_w + W_c; \quad V_w = W_w/F_w; \quad V_c = W_c/F_c. \quad (4)$$

We use (4) to represent the reduced velocity throughout the cross section as the weighted-mean one:

$$V = V_w \frac{F_w}{F} + V_c \frac{F_c}{F}. \quad (5)$$

From (1) together with (2) and (3) we get

$$V_w = V_c \left( \frac{\zeta}{\lambda} \cdot \frac{D}{d} \right)^{\frac{1}{2}}.$$

Then (5) may be put as

$$V = V_c \left( \frac{\zeta}{\lambda} \cdot \frac{D}{d} \right)^{\frac{1}{2}} \frac{F_w}{F} + V_c \frac{F_c}{F},$$

\*Deceased.

All-Union Scientific-Research Institute of Metallurgical Heat Engineering, Sverdlovsk. Translated from *Inzhenerno-Fizicheskii Zhurnal*, Vol. 22, No. 1, pp. 107-116, January, 1972. Original article submitted February 4, 1971.

© 1974 Consultants Bureau, a division of Plenum Publishing Corporation, 227 West 17th Street, New York, N. Y. 10011. No part of this publication may be reproduced, stored in a retrieval system, or transmitted, in any form or by any means, electronic, mechanical, photocopying, microfilming, recording or otherwise, without written permission of the publisher. A copy of this article is available from the publisher for \$15.00.

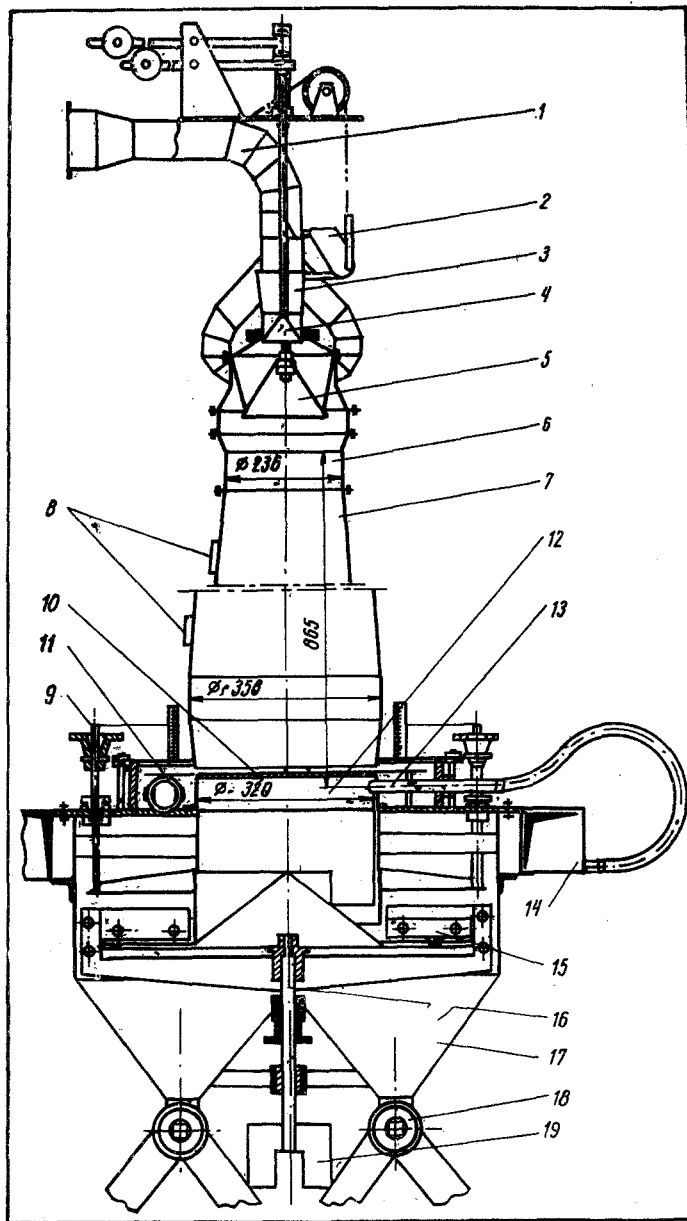


Fig. 1. Model of blast furnace (volume  $0.069 \text{ m}^3$ ): 1) common gas line, 2) skip; 3) receiving hopper; 4) small cone; 5) large cone; 6) charge hole; 7) column; 8) side temperature monitor; 9) feed screw; 10) supporting disk with holes; 11) horizontal strain gauge; 12) hearth; 13) air nozzle; 14) annular air inlet; 15) outlet; 16) cutter drive shaft; 17) receiver; 18) two-way distribution stopcock; 19) reduction gear.

whence

$$V_c = \frac{V}{\left(\frac{\xi}{\lambda} \cdot \frac{D}{d}\right)^{\frac{1}{2}} \frac{F_w}{F} + \frac{F_c}{F}} \quad (6)$$

We making the following two assumptions:

a) The coefficient for the aerodynamic resistance to the gas flow moving along the wall is proportional to the square of the coefficient of friction for the material at the wall, i.e.,

$$\lambda = K_1 f_w^2; \quad (7)$$

b) The relative area of the wall layer is represented by  $F_w/F$  and is proportional to the above geometrical ratio for the layer, i.e.,

$$\frac{F_w}{F} = K_2 \frac{d}{D}. \quad (8)$$

Then these assumptions give with (6) that

$$\Delta P_c = \zeta \frac{h}{D} \cdot \frac{\gamma}{2g} \frac{V^2}{\left[ 1 + \theta \left( \frac{d}{D} \right)^{\frac{1}{2}} \frac{1}{f_w} \right]^2}, \quad (9)$$

where

$$\theta = \left( \frac{\zeta}{K_1} \right)^{\frac{1}{2}} K_2; \quad \frac{F_c}{F} \approx 1.$$

The change in the pressure loss with wall roughness under otherwise equal conditions is defined by

$$\frac{\Delta P_1}{\Delta P_2} = \frac{\zeta_1}{\zeta_2} \left[ \frac{1 + \theta_2 \left( \frac{d}{D} \right)^{\frac{1}{2}} \left( \frac{1}{f_w} \right)_2}{1 + \theta_1 \left( \frac{d}{D} \right)^{\frac{1}{2}} \left( \frac{1}{f_w} \right)_1} \right]^2. \quad (10)$$

Consider the relative magnitude of the flow occurring in the part near the wall; the above relationships enable us to put that

$$W_{wl} = \left( \frac{\zeta}{\lambda} \cdot \frac{D}{d} \right)^{\frac{1}{2}} \frac{W - W_w}{F_c} F_w.$$

This expression is transformed to give finally that

$$\frac{W_w}{W} = \frac{\theta \left( \frac{d}{D} \right)^{\frac{1}{2}} \frac{1}{f_w}}{1 + \theta \left( \frac{d}{D} \right)^{\frac{1}{2}} \frac{1}{f_w}}. \quad (11)$$

The unknown quantity in (10) and (11) is  $\theta$ , which may be determined by experiment, where the coefficient of friction at the wall is a variable quantity. The ratio  $\zeta_1/\zeta_2$  may be replaced by the following expression [14, 15]:

$$\frac{\zeta_1}{\zeta_2} = \frac{1 - \varepsilon_1}{1 - \varepsilon_2} \left( \frac{\varepsilon_2}{\varepsilon_1} \right)^3. \quad (12)$$

The experiments were done with a cold model for a blast furnace (Fig. 1). Full details have been given elsewhere [16]. In place of the shaft of the blast furnace we had a cylindrical steel pipe of diameter 320 mm and height 890 mm; instead of the material loaded into the column we used loading via an intermediate funnel and grid (random loading). The speed of the material was constant at 12 mm/min in all cases. The wall roughness was provided by depositing electrotechnical graphite or fine-grained emery powder on the wall. The traveling medium was a coke in narrow fraction sizes: 2-3, 3-5, or 5-7 mm. We took into account the transient response time, which is involved in the structure alteration when the layer passes from the immobile state to the mobile one [17]. Table 1 gives the porosity and coefficient of friction at the wall.

We draw up a system of three equations for the immobile layer:

$$\frac{\Delta P_{g0}}{\Delta P_{e0}} = \frac{1 - \varepsilon_{g0}}{1 - \varepsilon_{e0}} \left( \frac{\varepsilon_{e0}}{\varepsilon_{g0}} \right)^3 \left[ \frac{1 + \theta_{e0} \left( \frac{d}{D} \right)^{\frac{1}{2}} \frac{1}{f_e}}{1 + \theta_{g0} \left( \frac{d}{D} \right)^{\frac{1}{2}} \frac{1}{f_g}} \right]^2,$$

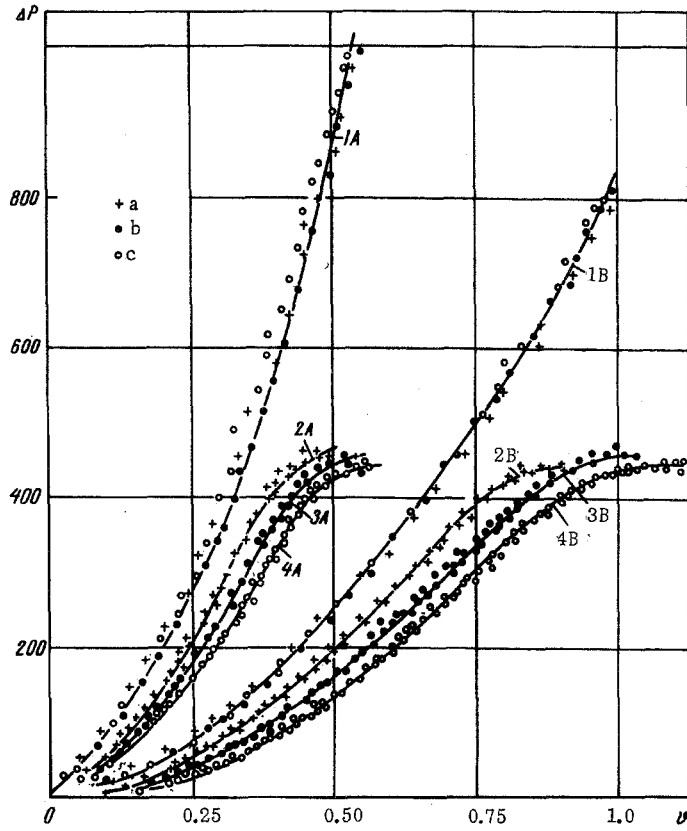


Fig. 2. Effects of wall friction on pressure loss  $\Delta P$  (mm) water as a function of air speed  $V$  (m/sec); A) coke 2-3 mm fraction; B) ditto 5-7 mm; 1) at rest; 2-4) moving, for  $f_w$  of: a) 0.39; b) 0.57; c) 0.80.

$$\frac{\Delta P_{g0}}{\Delta P_{s0}} = \frac{1 - \varepsilon_{g0}}{1 - \varepsilon_{s0}} \left( \frac{\varepsilon_{s0}}{\varepsilon_{g0}} \right)^3 \left[ \frac{1 + \theta_{s0} \left( \frac{d}{D} \right)^{\frac{1}{2}} \frac{1}{f_s}}{1 + \theta_{g0} \left( \frac{d}{D} \right)^{\frac{1}{2}} \frac{1}{f_g}} \right]^2, \quad (13)$$

$$\frac{\Delta P_{s0}}{\Delta P_{e0}} = \frac{1 - \varepsilon_{s0}}{1 - \varepsilon_{e0}} \left( \frac{\varepsilon_{e0}}{\varepsilon_{s0}} \right)^3 \left[ \frac{1 + \theta_{e0} \left( \frac{d}{D} \right)^{\frac{1}{2}} \frac{1}{f_e}}{1 + \theta_{s0} \left( \frac{d}{D} \right)^{\frac{1}{2}} \frac{1}{f_s}} \right]^2.$$

From the experimental data (curves 1A and 1B of Fig. 2) we find  $\Delta P_{g0} / \Delta P_{c0} = \Delta P_{g0} / \Delta P_{s0} = \Delta P_{s0} / \Delta P_{e0}$  for the immobile layer, so one can determine  $\theta$  for various coefficients of friction.

The value of  $\theta$  for a moving layer may be determined, for instance, from the following equation for a steel wall:

$$\frac{\Delta P_{s0}}{\Delta P_{sm}} = \frac{1 - \varepsilon_{s0}}{1 - \varepsilon_{sm}} \left( \frac{\varepsilon_{sm}}{\varepsilon_{s0}} \right)^3 \left[ \frac{1 + \theta_{sm} \left( \frac{d}{D} \right)^{\frac{1}{2}} \frac{1}{f_c}}{1 + \theta_{s0} \left( \frac{d}{D} \right)^{\frac{1}{2}} \frac{1}{f_c}} \right]^2. \quad (14)$$

Here  $f_s$  remains constant for immobile and mobile layers, in accordance with the above assumption.

In (14), we take the ratio of the pressure loss for the immobile and mobile layers in accordance with Fig. 2 (curves 2A-4A and 2B-4B), but for an infiltration rate not exceeding the limiting value, i.e., a speed at which there was no additional expansion of the layer in response to the lifting forces of the rising gas flow [18].

TABLE 1. Effects of Wall Friction on Bed Characteristics

Coating and coefficient of friction $f_w$	Coke fraction, mm																			
	2-3				3-5				5-7											
	stationary bed		moving bed		stationary bed		moving bed		stationary bed		moving bed									
	$\epsilon_0$	$\left(\frac{W_w}{W}\right)_0$	$\epsilon_m$	$\theta_m \left(\frac{W_w}{W}\right)_m$	$\epsilon_0$	$\left(\frac{W_w}{W}\right)_0$	$\epsilon_m$	$\theta_m \left(\frac{W_w}{W}\right)_m$	$\epsilon_0$	$\left(\frac{W_w}{W}\right)_0$	$\epsilon_m$	$\theta_m \left(\frac{W_w}{W}\right)_m$								
Graphite $f_w = 0.30-0.40$	0,36	1,27	0,22	0,40	1,00	0,18	0,33	1,51	0,36	1,51	0,33	0,40	1,18	0,27	0,41	1,73	0,37	0,45	1,60	0,35
Untreated steel $f_w = 0.55-0.58$	0,36	1,50	0,19	0,40	1,50	0,19	0,27	1,88	0,37	1,88	0,27	0,41	1,94	0,28	0,42	2,30	0,36	0,45	2,30	0,36
Fine-grained emery $f_w = 0.78-0.82$	0,37	1,60	0,16	0,41	2,25	0,20	0,22	2,01	0,38	2,01	0,22	0,42	2,96	0,29	0,43	2,76	0,32	0,47	3,84	0,40

We solve (13) and the three analogous equations of (14) to get  $\theta$  for all cases of interest (see Table 1).

Table 2 gives the observed and calculated changes in the pressure loss for the coke in the various fractions in the immobile and mobile beds; Equation (11) gave the proportion of the flow in the part near the wall.

Table 1 shows that the porosity of the granular layer increases with the coefficient of friction; for an immobile and finely divided material, there is a rise in the porosity to a smaller extent than that found with a moving coarse-grained material, which means that the pressure loss will be reduced when the layer is mobilized and when the coefficient of friction at the wall increases (whether the layer is immobile or mobile). On the other hand, increase in the coefficient of friction changes the distribution of the gas flux over the radius of the layer; in an immobile layer there is a reduction in the flow near the wall, while in a counterflow case there is a rise (Table 1).

A rise in the gas flow nonuniformity due to the radial structure of the granular layer is accompanied by a reduction in the overall pressure loss; flow equalization results in an increase in the loss.

Porosity increase and reduction in flow nonuniformity for an immobile layer cause the pressure loss as a function of coefficient of friction to be represented essentially by a single curve (Fig. 2); in the case of countercurrent flow, the two factors, (increased porosity and nonuniform velocity distribution) together facilitate reduction in the pressure loss. The part of Fig. 2 for countercurrent flow is clearly represented by three curves corresponding to the different coefficients of friction at the wall.

Table 1 also shows that the exact magnitude of the flow nonuniformity increases with the grain size and remains substantial even when  $d/D$  is less than 0.01.

It is clear from the experiments and calculations that increased wall roughness reduces the nonuniformity in the air distribution along a radius when the layer is immobile, whereas one gets an increase in the nonuniformity when we have a countercurrent situation.

We made tests on the partition of the flow over the radius for immobile and mobile layers with various wall roughnesses for this apparatus by the method of [19]; the entire cross section of the bed was divided into five concentric zones equal in area. Around the circumference of each zone we placed 38 naphthalene spheres of diameter close to the linear diameter of the bed grains. The height of the zone where the spheres were emplaced was 850 mm above the zone of flow stabilization near the bottom, the level of this being 1/8 of the radius of the bed.

Figure 3 shows in relative coordinates the average results for several runs with the two states of motion and various wall roughnesses; the general trends in the curves agree well with the results considered above. There is a nonuniformity in the air speed along the radius for the immobile bed (curve 2), which becomes more marked when the bed begins to move (curve 4). The maximum in the air flow speed also moves towards the wall.

TABLE 2. Observed and Calculated Pressure Losses for Countercurrent Flow with Rough Walls

Coke fraction	Pressure loss change			Notes
	$\frac{\Delta P_{gm}}{\Delta P_{em}}$	$\frac{\Delta P_{gm}}{\Delta P_{sm}}$	$\frac{\Delta P_{sm}}{\Delta P_{em}}$	
2-3	1,20	1,09	1,13	Obs
	1,19	1,06	1,11	Calc
3-5	1,21	1,08	1,15	Obs
	1,23	1,09	1,12	Calc
5-7	1,27	1,08	1,17	Obs
	1,24	1,05	1,19	Calc

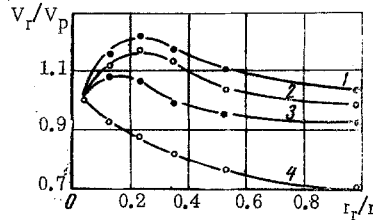


Fig. 3. Relative distribution of flow velocity over radius of layer of coke fraction 5-7 mm: 1) immobile layer, graphite wall; 2) emery wall; 3) mobile layer, graphite wall; 4) emery wall ( $V_p$ : value of flow velocity at periphery;  $V_r$  running value;  $r$ : radius of layer;  $r_r$ : running value of radius).

The overall characteristics were used to calculate the actual change in air speed when the immobile layer is set in motion (for the case of a wall covered with emery).

The amount of material evaporating from the surface of a grain in unit time is proportional to the gas flow speed  $V$  and the mass-transfer surface  $S$  [19]:

$$\Delta q = KSV^{1/n}, \quad (15)$$

where  $n$  is a quantity characterizing the mode of motion; it follows from (15) that

$$\frac{\Delta q_0}{\Delta q_m} = \frac{KSV_0^{1/n}}{KSV_m^{1/n}}. \quad (16)$$

The test was run as follows. Air was blown through immobile and mobilized beds of 2-3 mm coke for an hour at the same blower output; the weight loss in the naphthalene spheres (of identical size in both cases) was larger by a factor 2.3 for the immobile bed, and we had from (16) that

$$2.3 = (V_0/V_m)^{1/n}.$$

We had  $m = 0.67$  for  $Re = 144$  under the conditions used.

Then the following is the change in the actual air flow speed when the bed is mobilized, as averaged over the radius:

$$V_0/V_m = 1.75.$$

This fall in the speed is due to increase in the porosity and effects of the increasing nonuniformity in the velocity distribution when the bed is mobilized.

Thus the wall roughness has a marked effect on the structure of a countercurrent layer, which is reflected in the change in the pressure loss, as well as in the velocity distribution and in the behavior of the gas along the radius. All of these factors should have an appreciable effect on the heat and mass transfer in such a system.

When one is using models for a countercurrent process, one must take into account the wall roughness as regards the final results not only by meeting the requirement  $(d/D)_{nat} = (d/D)_{mod}$  but also by meeting the specification  $(f_w)_{nat} = (f_w)_{mod}$ .

## NOTATION

$\Delta P$	is the pressure loss;
$V$	is the reduced gas flow velocity;
$D$	is the diameter of the layer;
$d$	is the characteristic dimension of the particles;
$F$	is the cross-sectional area of the layer;
$W$	is the amount of gas;
$h$	is the height of the layer;
$\gamma$	is the specific weight of the gas;
$f_w$	is the coefficient of friction at the wall;
$\lambda, \xi$	are the aerodynamic resistance coefficients for the air moving along the wall and in the layer, respectively;
$\varepsilon$	is the porosity of the layer;
$g$	is the acceleration due to gravity.

### Subscripts

w	denotes the wall;
c	denotes the central part of the layer;
p	denotes the peripheral part of the layer;
g	denotes the graphite wall;
s	denotes the steel wall;
e	denotes the emery wall;
o	denotes the immobile layer;
m	denotes the mobile layer.

## LITERATURE CITED

1. A. N. Chernyatin, Proceedings of the Ural Polytechnical Institute [in Russian], No. 73, Metallurgizdat, Moscow-Sverdlovsk (1958), pp. 87-105.
2. M. Kimura, K. Mowo, and T. Kaneda, Chem. Eng. Japan, 19, 397 (1960).
3. R. F. Benenati and G. B. Broilow, Am. Inst. Chem. Eng. Jour., 8, 359 (1962).
4. H. Rumpf, S. Dellas, and K. Shonert, Chem. Ind. Techn. 39, 116 (1967).
5. N. M. Zhavoronkov, M. É. Aérov, and N. N. Umnik, Zh. Fiz. Khim., 23, No. 3 (1949).
6. G. K. Boreskov and L. G. Ritter, Khim. Prom., No. 6 (1946).
7. P. N. Grekov, Izv. VUZ. Chernaya Metallurgiya, No. 9 (1965).
8. P. I. Luk'yanov, N. V. Gusev, and N. I. Nikitina, Khim. i Tekh. Topliv i Masel, No. 12 (1957).
9. M. E. Bernshtein and A. G. Immerman, Researches on Bulk and Rod Constructions [in Russian], GILSA, Moscow (1952), pp. 183-223.
10. Ernst, Express Information: Chemical Plant and Processes [in Russian], No. 16, VINITI (1960).
11. R. A. Findley and R. G. Hoynes, Recent Advances in Oil Refining and Petrochemistry [Russian translation], Vol. 2, Gostoptekhizdat (1961).
12. Z. R. Gorbis, Heat Transfer and Hydromechanics of Dispersed Transverse Flows [in Russian], Énergiya, Moscow (1970).
13. V. A. Borisevich, Trudy Inst. Énergetiki AN BSSR, issue 11, Izd. AN BSSR (1960), pp. 17-26.
14. J. Happel, Ind. Eng. Chem., 41, No. 6, 1161 (1949).
15. N. V. Kel'tsev, Gaz. Prom., No. 12 (1957).
16. V. K. Durnov, Nauch. Trudy VNIIMT, Vol. 20, Metallurgiya, Moscow (1970), pp. 23-40.
17. V. K. Durnov, Nauch. Trudy VNIIMT, Vol. 20, Metallurgiya, Moscow (1970), pp. 61-76.
18. V. K. Durnov, Nauch. Trudy VNIIMT, Vol. 20, Metallurgiya, Moscow (1970), pp. 77-91.
19. M. É. Aérov and N. N. Umnik, Zh. Prikl. Khim., 28, No. 6 (1955).